


## RESEARCH ARTICLE

# Molecular dynamics characterization of silver colloidal interfaces for SERS applications. Gallic acid test

D. Muñoz-Gacitúa<sup>1</sup>  | C. Garrido<sup>2</sup> | A. Ruiz-Fernández<sup>1</sup> | H. Ahumada<sup>3</sup> |  
M. M. Campos-Vallette<sup>2</sup> | R. Araya-Maturana<sup>4</sup> | B. E. Weiss-López<sup>1</sup>

<sup>1</sup>Laboratorio de Físicoquímica Molecular, Facultad de Ciencias, Universidad de Chile, Santiago, Chile

<sup>2</sup>Laboratorio de Espectroscopía Vibracional, Facultad de Ciencias, Universidad de Chile, Santiago, Chile

<sup>3</sup>Laboratorio de Química Biotecnología y Productos Naturales, Departamento de Ciencias Básicas, Facultad de Ciencias, Universidad del Bio Bio, Chillan, Chile

<sup>4</sup>Instituto de Química y Recursos Naturales, Universidad de Talca, Talca, Chile

## Correspondence

B. E. Weiss-López, Laboratorio de Físicoquímica Molecular, Facultad de Ciencias, Universidad de Chile, Santiago, Chile.

Email: bweiss@uchile.cl

## Funding information

Fondo Nacional de Desarrollo Científico y Tecnológico (FONDECYT), Grant/Award Number: 1150138; Comisión Nacional de Investigación Científica y Tecnológica (CONICYT), Grant/Award Number: 212832

## Abstract

One of the most useful applications of silver colloidal solutions is in surface-enhanced Raman spectroscopy (SERS), because the amplification factor of about  $10^6$  allows the vibrational study and detection of highly diluted species in aqueous environment, and more recently in early diagnosis of cancer and imaging. A useful colloid for SERS is that reported by Leopold and Lendl (Colloid 1). However, SERS response from anions or rich electron density molecules has been difficult to obtain in this colloid. Recently, a minor modification of the surface charge density (Colloid 2) allowed to observe reproducible SERS spectrum from gallate anion ( $\text{GA}^-$ ). In this work, the structure of both solid and solution interfaces were characterized using molecular dynamics. Experimental values of  $\zeta$ -potentials were reproduced by simulations, and the chemical potential of  $\text{GA}^-$  approaching both interfaces was calculated using “umbrella sampling” and the weighted histograms analysis methodology (WHAM). The calculated barrier to approach the interface of Colloid 1 is  $2.8 \text{ kJmol}^{-1}$  greater than in Colloid 2, and the stability of  $\text{GA}^-$  with Colloid 2 at the minimum is  $3.5 \text{ kJmol}^{-1}$  more stable than with Colloid 1. Finally, the calculated average orientation of  $\text{GA}^-$  adsorbed onto the colloidal surface is in excellent agreement with the experimental SERS observations.

## KEYWORDS

gallic acid, molecular dynamics, SERS, silver colloid, umbrella sampling

## 1 | INTRODUCTION

Silver colloids consist of a dispersion of nanometric silver particles suspended in some solvent, usually water, and depending on preparation the particles can have different shapes and sizes. The suspension is stabilized by electrostatic repulsions among the particles. These solutions are usually prepared by partial reduction of a water soluble silver salt, such as silver nitrate, to metallic silver, by a reducing agent such as  $\text{NaBH}_4$ , sodium citrate, hydroxylamine hydrochloride ( $\text{HXA.HCl}$ ), and sugars.<sup>[1, 2]</sup> The nonreduced silver ions that remain charged guarantee the stability of the suspension. In the presence of counter-ions,

such as chloride, an electric double layer at the nanoparticle surface is formed, with a Stern and diffuse layers of counter-ions.

A commonly employed methodology to characterize the colloidal particle surface charge is to measure  $\zeta$ -potentials,<sup>[3]</sup> defined as the necessary work to bring a positive charge from infinity to the proximity of the diffuse layer.  $\zeta$ -potentials can be experimentally measured using light scattering. This property has been associated to the stability of the colloidal solution, and nanoparticles with  $\zeta$ -potentials more positive than  $+30 \text{ mV}$  or more negative than  $-30 \text{ mV}$  are usually considered stable.<sup>[3]</sup>

For centuries, silver colloidal solutions have been used in the treatment of infections due to bacteria, parasites, and viruses, including AIDS. However, there is no conclusive evidence of health benefits and the risk involved in consumption exceeded by far the possible benefits. More recently, silver nanoparticles are employed in domestic appliances, such as freezers, washing machines, wool manufacturing, and sensing devices.<sup>[4–9]</sup>

Among the most interesting applications of silver colloids are the vibrational analysis and identification of molecules at traces concentration levels in water and, more recently, in-vivo diagnostics of cancer at early stages of tumor development,<sup>[10]</sup> both by using surface-enhanced Raman spectroscopy (SERS). In effect, the coupling of the plasmon resonance of the silver particle with the inelastic scattering between the photon and the elements of the molecular polarizability tensor produces an enhancement of the Raman signal in the order of  $10^6$ . A commonly used colloid in SERS applications is that reported by Leopold and Lendl<sup>[11]</sup> (Colloid 1), prepared by reduction of silver nitrate with an excess of HXA.HCl. It makes possible the identification and vibrational studies of extremely diluted species, such as biologically interesting molecules in aqueous environment, where using other methodologies is more difficult. In favorable cases, applying SERS selection rules, it is possible to estimate the orientation of the analyte adsorbed on the nanoparticle surface.<sup>[12]</sup>

It is not always possible to obtain SERS spectrum from a given analyte. Particularly, rich electron density or anionic molecules usually do not display SERS spectrum when dissolved in Colloid 1, possibly due to repulsive electrostatic interactions between chlorides at the Stern layer and the electron density on the molecule. A couple of attempts to obtain SERS response from gallate anion ( $GA^-$ ) in silver colloids have been made without any success.<sup>[13, 14]</sup> Furthermore, SERS response from  $GA^-$  dissolved in Colloid 1 has been impossible to obtain. The fact that  $GA^-$  carries a net negative charge, in addition to contain several atoms with lone pair electrons, imposes restrictions to the approximation of this type of molecules to the silver nanoparticle surface. In a recent study,<sup>[15]</sup> it was shown that by employing less amount of reducing agent, it is possible to obtain a modified colloidal solution (Colloid 2) with a smaller negative surface charge. In effect, Colloid 1 has a  $\zeta$ -potential of  $-43 + -2$  mV, whereas Colloid 2 displays a  $\zeta$ -potential of  $-31 + -3$  mV. The new preparation has less negative surface charge than the original one, due to the less amount of chloride ions available. Colloid 2 allowed to obtain good SERS spectral reproducibility in several negatively charged molecules. Even more, from a close examination of the intensities and shifts of the vibrational frequencies, it was possible to estimate

the orientation of the aromatic ring of  $GA^-$  relative to the colloidal particle surface plane.<sup>[16]</sup>

In this work, we present a molecular dynamics (MD) simulation study of the two silver colloid interfaces described before. The interfaces were represented by a silver particle in the (1,1,1) crystal structure, surrounded by an aqueous sodium chloride (NaCl) solution. In order to validate the simulations of the colloidal interfaces, we have explored the silver particle charge and the ionic strength, to reproduce the experimentally measured values of  $\zeta$ -potentials. Properties to characterize both colloid interfaces were calculated. Finally, in order to provide an explanation to the experimental observations, “umbrella sampling/Wham” methodology<sup>[17, 18]</sup> was employed to calculate the chemical potential for the process of approaching  $GA^-$  towards both interfaces. The results of this study reproduce the experimental observations, including the orientation of the anion in the particle surface, providing a detailed picture of the reorientational process experienced by  $GA^-$  as a consequence of the electrostatic potential generated by the silver nanoparticle charge and the ionic aqueous solution.

## 2 | MOLECULAR DYNAMICS

All MD trajectories and further analysis were performed employing the software bundle GROMACS 5.0.5, with the GROMOS56a7 force field,<sup>[19, 20]</sup> including Lennard-Jones parameters for silver. These parameters were obtained by Heinz et al.<sup>[21]</sup> by fitting the surface tension and density of a (1,1,1) silver crystal at 300K.  $GA^-$  was included as sodium gallate in the simulation, and its partial charges were assigned based on a *ab-initio* HF/6-311G\* geometry optimization and Mulliken electron population analysis, and the results are shown in Figure 1.

A computer-generated box of dimensions 2.84, 2.84, and 12.0 nm in the X, Y, and Z directions, respectively, containing a (1,1,1) silver crystal consisting of 4 layers of 98 silver atoms each in the XY plane, was constructed. In order to have symmetric interfaces in both sides of the crystal, the generated structure was copied, rotated 180° through X, and displaced along Z to finally obtain eight layers containing 784 atoms in a (1,1,1) silver crystal structure, 2.0 nm width, with interfaces at  $Z = 0.0$  nm and  $Z = -2.0$  nm. Two percent of the silver atoms were randomly selected to be replaced with positive silver ions, this random selection was biased to charge more atoms at the surface than inside the metal. The empty space of the box was filled with 2,697 simple point charge (SPC/E) water molecules,<sup>[22]</sup> and sodium and chloride ions were added at different concentrations in order to neutralize all charges and provide ionic strength. To avoid surface effects,

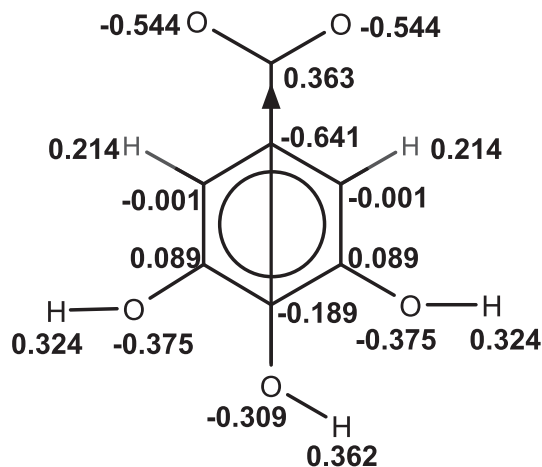


**FIGURE 1** Gallate molecule with its partial charges according to a Mulliken population analysis. The arrow represents the  $C_2$  axis

periodic boundary conditions were employed in all directions of space. Long range electrostatic interactions were calculated using Particle Mesh Ewald method<sup>[23]</sup> with a cutoff of 1.4 nm, and the same cutoff was employed for the Lennard–Jones potential. The time step size in all simulations was 2 fs. To avoid bad contacts, after the boxes were assembled, the energy was minimized until there were no interaction forces greater than  $1,000 \text{ kJmol}^{-1} \text{ nm}^{-1}$ . After that, the temperature was adjusted using the Berendsen thermostat<sup>[24]</sup> in the canonical ensemble, and the pressure controlled by using the Parinello-Rahman algorithm,<sup>[25]</sup> in the isothermic-isobaric ensemble. Then, 13 isothermic-isobaric trajectories of 210 ns each, at different surface charges and salt concentrations, were calculated. An equilibration time of 10 ns was allowed for each simulation, and they were discarded for any further analysis. In addition, to understand the observed differences at molecular level, chemical potential profiles for the process of approaching  $GA^-$  towards both colloidal interfaces were obtained using the umbrella sampling/WHAM methodology. Simulation windows of 20 and 23 were calculated for Colloids 1 and 2, respectively, all with 30 ns trajectories in the canonical ensemble. The force constant employed to restraint the position of  $GA^-$  in each window was  $1,000 \text{ N/m}$ , whereas the force constant for the pulling process to generate the windows was  $300 \text{ N/m}$ .

### 3 | RESULTS AND DISCUSSION

#### 3.1 | Calculation of $\zeta$ potential

The main purpose of this paper is to find an explanation to the differences observed between the behavior of Colloids 1 and 2, related to the difficulties associated with the observation of SERS response from anionic or high electron density analytes. To achieve this goal, a series of MD

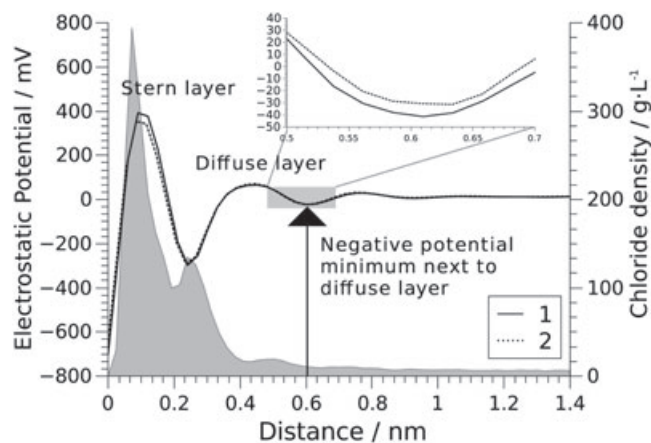


**FIGURE 2** Electrostatic potential (black and dotted lines) and chloride density on Colloid 2 (shaded area) vs distance from the interface in a molecular dynamics simulation of a silver colloid surface

simulations were performed. To validate the simulations, we have explored the charge of the nanoparticle and the ionic strength of the solution, to reproduce the experimentally measured  $\zeta$ -potentials,  $-43 \pm 2 \text{ mV}$  and  $-31 \pm 3 \text{ mV}$  for Colloids 1 and 2, respectively. To identify the distance at which  $\zeta$ -potentials had to be measured, a calculation of the electrostatic potential profile of a positive charge perpendicularly approaching the surface was performed from a 200-ns trajectory. Mass density profile of chloride ions along the Z-axis of the box was also calculated from the same trajectory. Figure 2 shows a superposition of both results.

Closely packed to the surface, a layer of chloride ions of about 0.2-nm thick can be observed; this corresponds to the Stern layer, formed by counter-ions adsorbed on the silver surface. Further away, it is possible to find the diffuse layer, by the end of it, a region of negative potential. This point corresponds to the distance at which  $\zeta$ -potential has to be measured. This figure clearly evidences the existence of an electric double-layer structure at the surface.

Therefore, knowing the distance at which  $\zeta$ -potentials have to be measured, an exploration about the dependence of this potential with nanoparticle charge, at constant ionic strength (0.1M NaCl), was conducted. Figure 3 is a plot of these results.

An inspection to this figure reveals that the simulation with 2% charged silver atoms and 0.1M NaCl gives a  $\zeta$ -potential of  $-30 \pm 3 \text{ mV}$ , very close to the experimental value of Colloid 2,  $-31 \pm 3 \text{ mV}$ . Therefore, the 2% silver ions crystal was chosen to be representative of the colloidal particle charge.

After that, a study concerning the dependence of  $\zeta$ -potential with ionic strength, at constant silver ions percentage, was conducted. Simulations with NaCl concentrations from 0.1M to 0.36M were performed, and

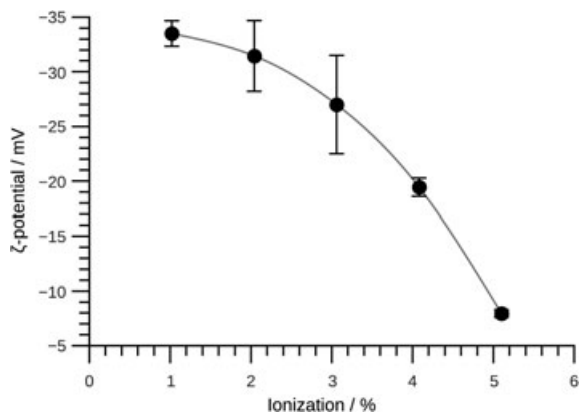


**FIGURE 3**  $\zeta$ -potential vs percentage of ionized silver atoms from molecular dynamics simulations

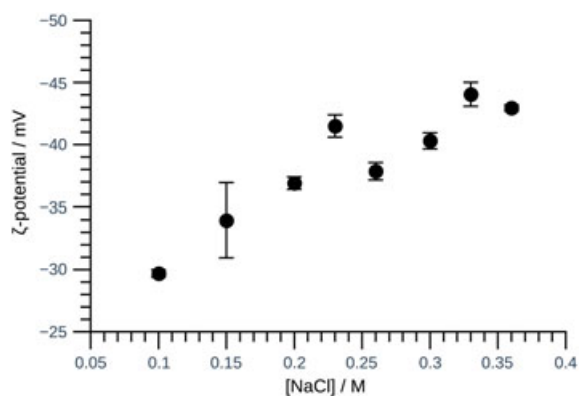


**FIGURE 4**  $\zeta$ -potential vs NaCl concentration in molecular dynamics simulations of the silver surface from Colloid 2 [Colour figure can be viewed at [wileyonlinelibrary.com](http://wileyonlinelibrary.com)]

$\zeta$ -potentials were calculated. The results are plotted in Figure 4. This figure shows, as expected, that  $\zeta$ -potential becomes more negative with the increase in ionic strength. It can also be observed that the simulation with NaCl 0.23M displays a  $\zeta$ -potential of  $-41 \pm 1$  mV, close to the experimental value from Colloid 1,  $-43 \pm 2$  mV. Therefore, simulations with 2% silver ions in the crystal, immersed in 0.23M and 0.10M NaCl solutions, reproduce the experimental  $\zeta$ -potentials and are representatives of Colloids 1 and 2, respectively.

After validation of both simulations by reproducing the experimental  $\zeta$ -potentials, electrostatic potentials for both silver interfaces, from 1.5 nm away, were calculated, and the results are shown in Figure 2. Both potential profiles are very similar, not a surprise considering that the only difference between them arises from the ionic strength. The main difference comes from an energy barrier at about 0.13 nm away from the silver surface. This barrier arises mainly from the structure of water molecules and counter-ions near the interface. Water molecules at the interface are not like the ones at the bulk of the solution.

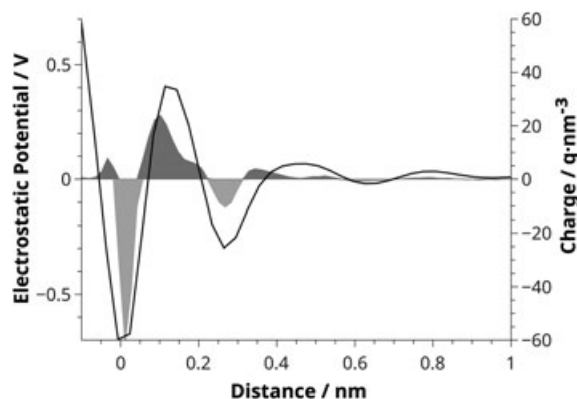


**FIGURE 5** Electrostatic potential (black line) and water charge density (shaded area) vs distance from the interface in a molecular dynamics simulation of Colloid 2

Water possesses a strong electric dipole moment, and at the nanoparticle surface, it becomes, on average, oriented with the high electron density from the oxygen atom towards the positive silver crystal, and the positive end in the opposite direction. Figure 5 shows the calculated charge density of water dipoles along the Z-axis of the simulation box. In effect, a distribution of oriented water dipoles near the interface is clearly observed. Even more, from the same figure, two zones of water dipole polarization can be distinguished near the silver surface, around the Stern layer, the one just mentioned before, and a second zone near the diffuse layer, with significant less order. At distances greater than 0.5 nm the distribution of dipoles is random. This ordering is the main responsible for the increase in electrostatic potential, because there is a region of excess positive charge due to the protons from the solvent. The excess of charges in the Stern layer of Colloid 1 compared with Colloid 2 contributes to this ordering, increasing electrostatic interactions.

### 3.2 | Chemical potential of $GA^-$ approaching the silver surface

At  $pH = 5$ , gallic acid is completely dissociated, and the only species in solution, and consequently, the only one adsorbed in the colloidal particle is  $GA^-$ . SERS response from  $GA^-$  dissolved in Colloid 1 has been impossible to obtain. However, SERS spectrum from  $GA^-$  adsorbed in Colloid 2 has been recently obtained with good reproducibility.<sup>[16]</sup> Several band intensity variations and wavenumber shifts, relative to the Raman spectrum, were observed and are consistent with an orientation of the aromatic ring perpendicular to the interface, with the  $COO^-$  moiety pointing towards the positively charged silver surface.<sup>[16]</sup>

In order to provide an atomic level understanding about the origin of the observed differences in behavior of both

colloidal solutions in the presence of  $GA^-$ , the chemical potential profile for the process of perpendicularly approaching  $GA^-$  towards both interfaces were calculated. To perform these calculations, the umbrella sampling/WHAM methodology was employed.<sup>[26]</sup>

To perform the chemical potential calculation, it was necessary to incorporate  $GA^-$  into the computational box, and this was done by first eliminating all water molecules, then incorporating  $GA^-$ , and finally adding water molecules again. After that, the system is subjected to energy minimization cycle, identical to the ones previously described. Then, 100 ns MD trajectory calculations of free  $GA^-$  in both interfaces were performed. After few nanoseconds of trajectory,  $GA^-$  spontaneously becomes adsorbed into both colloidal particle interfaces.

The main question of this paper is that what makes Colloid 2 to adsorb  $GA^-$ . To provide a quantitative answer to this question, both chemical potential profiles were calculated. The results of these calculations are displayed in Figure 6. From this figure, it is observed that, as expected, at long distances, there is no significant interaction between the interface and  $GA^-$ ; however, at distances smaller than 0.5 nm, the effect of the electrostatic potential from the interface begins to be experienced by the anion. At about 0.14 nm, a local minimum and an energy barrier are clearly observed, to finally reach the global minimum. Because the largest energy barrier to be surmounted in the adsorbing process is the one just mentioned, it will determine the rate of the process. Figure 6 also shows an expansion of that region of interest. From this figure, it is clearly observed that the activation energy barrier for the process of approaching Colloid 1 interface is +2.8 kJ/mol higher than for the case of Colloid 2. Furthermore,  $GA^-$  adsorbed on Colloid 2 interface is 3.6 kJ/mol more stable

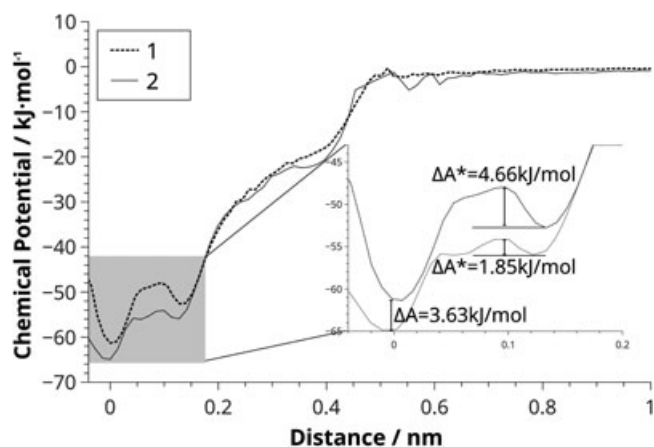


**FIGURE 6** Chemical potential for the approaching  $GA^-$  onto both colloidal surfaces. Colloid 1 is shown as a dotted line, and Colloid 2 as a continuous one

than adsorbed in Colloid 1. Therefore, there are two phenomena that favor the adsorption of  $GA^-$  in Colloid 2, first, a kinetic effect from the rate determining step and, second, a thermodynamic effect, provided by the higher stability of the adsorbed species.

The minimum observed at 0.13 nm arises mainly from the interaction of  $GA^-$  with the protons from the oriented solvent molecules, and the barrier is for the process of crossing the Stern layer of chlorides. Obviously, Colloid 1 contains more chlorides at the interface and displays a high activation energy barrier. Figure 7 is a superposition of the charge distribution of water dipoles (shaded area) and the chemical potential profile (black line).

In this plot, it is observed that this dipole charge distribution is strongly influenced the shape of the chemical potential. In an effort to reveal details about the mechanism of adsorption in Colloid 2, the orientation of the  $C_2$  symmetry axis of  $GA^-$  (see Figure 1) with respect to the Z-axis of the box, perpendicular to the silver

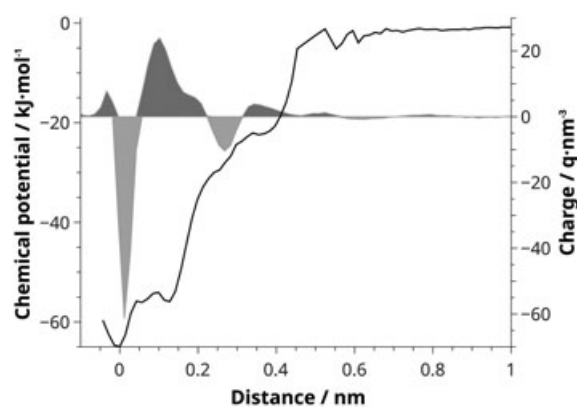


**FIGURE 7** Chemical potential (black line) and water charge density (shaded area) vs. distance from the interface in a MD simulation of Colloid 2

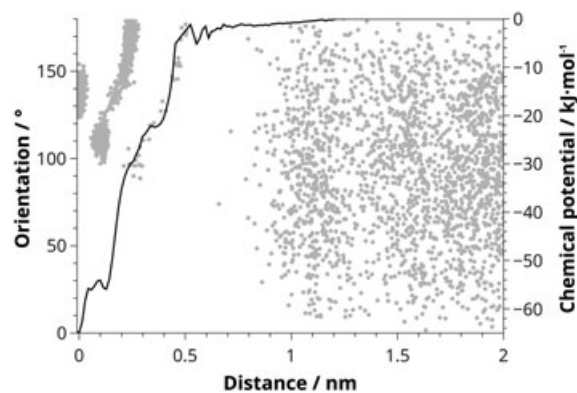


**FIGURE 8** Chemical potential for the approaching gallate onto Colloid 2 and orientation of its  $C_2$  symmetry axis with respect to the Z axis (perpendicular to the silver plane) vs. distance from the interface

surface, was plotted and superimposed with the chemical potential calculation. This plot is displayed in Figure 8 and is observed that further away from 0.7 nm, the charge density of the interface has no clear effect on the orientation of  $GA^-$ . However, at closer distances, it adopts different orientations, including perpendicular to the Z-axis. This particular orientation arises from interactions between the ring delocalized negative charge with positive charge density from the oriented water molecules, similar to a cation- $\pi$  interaction.<sup>[27]</sup> Finally, the ring adopts an average orientation consistent with an angle of about 140° between the symmetry axis and the normal to the bilayer interface, in agreement with the experimental SERS observations.

## 4 | CONCLUSIONS

MD simulations have proven to be an extremely useful tool for the interpretation of colloidal interface behavior and their interactions with dissolved analytes.

Previously obtained SERS spectrum of gallic acid along with SERS selection rules, allowed to propose that  $GA^-$  is oriented on the surface with their symmetry axis perpendicular to the silver surface, with the  $COO^-$  fragment driving the interaction, in agreement with simulation results. The electrostatic potential of the solution is dominated by the distribution of water dipoles in it. Two phenomenon contribute to the observed differences, a kinetic contribution, from differences in activation energy, and a thermodynamic contribution, from differences in stability of the system. Finally, all the experimental evidence, including the orientation, is well reproduced by the simulation.

## ACKNOWLEDGEMENTS

The authors acknowledge financial support from FONDECYT, grant 1150138. D.Muñoz-Gacitúa acknowledges a doctoral fellowship from CONICYT, grant 212832. The authors also acknowledge the assistance from the staff and facilities at the National Laboratory for High Performance Computing (NLHPC) at Universidad de Chile.

## ORCID

D. Muñoz-Gacitúa  <http://orcid.org/0000-0001-9631-1572>

## REFERENCES

- [1] J. Lyklema, H. P. van Leeuwen, M. Vliet, A. M. Cazabat, *Fundamentals of Interface and Colloid Science: Fundamentals*, Academic Press, Cambridge, Massachusetts **1991**.
- [2] V. K. Sharma, R. a. Yngard, Y. Lin. *Adv. Colloid Interface Sci.* **2009**, *145*(1-2), 83.
- [3] R. J. Hunter, *Zeta Potential in Colloid Science: Principles and Applications*, Colloid science, Academic Press **1981**.
- [4] M. C. Fung, D. L. Bowen. *J. Toxicol. Clin. Toxicol.* **1996**, *34*(1), 119.
- [5] A. Panacek, L. Kvitek, R. Prucek, M. Kolar, R. Vecerova, N. Pizúrova, V. K. Sharma, T. Nevecna, R. Zboril. *J. Phys. Chem. B* **2006**, *110*(33), 16248.
- [6] M. Ahamed, M. S. AlSalhi, M. K. J. Siddiqui. *Clinica Chimica Acta* **2010**, *411*(23-24), 1841.
- [7] T. M. Tolaymat, A. M. El Badawy, A. Genaidy, K. G. Scheckel, T. P. Luxton, M. Suidan. *Sci. Total Environ.* **2010**, *408*(5), 999.
- [8] X. Chen, H. J. Schluesener. *Toxicol. Lett.* **2008**, *176*(1), 1.
- [9] Q. Li, S. Mahendra, D. Y. Lyon, L. Brunet, M. V. Liga, D. Li, P. J. J. Alvarez. *Water Res.* **2008**, *42*(18), 4591.
- [10] X. Qian, X. H. Peng, D. O. Ansari, Q. Yin-Goen, G. Z. Chen, D. M. Shin, L. Yang, A. N. Young, M. D. Wang, S. Nie. *Nat. Biotechnol.* **2007**, *26*(1), 83.
- [11] N. Leopold, B. Lendl. *J. Phys. Chem. B* **2003**, *107*(24), 5723.
- [12] M. Moskovits. *Rev. Mod. Phys.* **1985**, *57*(3), 783.
- [13] M. Leona, J. Stenger, E. Ferloni. *J. Raman Spectrosc.* **2006**, *37*(10), 981.
- [14] M. C. Alvarez-Ros, S. Sánchez-Cortés, O. Francioso, J. V. García-Ramos. *J. Raman Spectrosc.* **2001**, *32*(2), 143.
- [15] C. Garrido, B. E. Weiss-López, M. M. C. Vallette. *Spectrosc. Lett.* **2016**, *49*(1), 11.
- [16] C. Garrido, G. Diaz-fleming, M. M. Campos-vallette. *Spectrochemical Acta, Part A* **2016**, *163*, 68.
- [17] S. Kumar, J. M. Rosenberg, D. Bouzida, R. H. Swendsen, P. A. Kollman. *J. Comput. Chem.* **1992**, *13*(8), 1011.
- [18] J. S. Hub, B. L. De Groot, D. Van Der Spoel. *J. Chem. Theory Comput.* **2010**, *6*(12), 3713.
- [19] C. Oostenbrink, A. Villa, A. E. Mark, W. F. Van Gunsteren. *J. Comput. Chem.* **2004**, *25*(13), 1656.
- [20] D. Van Der Spoel, E. Lindahl, B. Hess, G. Groenhof, A. E. Mark, H. J. C. Berendsen. *J. Comput. Chem.* **2005**, *26*(16), 1701.
- [21] H. Heinz, R. a. Vaia, B. L. Farmer, R. R. Naik. *J. Phys. Chem. C* **November 2008**, *112*(44), 17281.
- [22] H. J. C. Berendsen, J. R. Grigera, T. P. Straatsma. *J. Phys. Chem.* **1987**, *91*(24), 6269.
- [23] P. P. Ewald. *Annalen der Physik* **1921**, *369*(3), 253.
- [24] H. J. C. Berendsen, J. P. M. Postma, W. F. van Gunsteren, A. DiNola, J. R. Haak. *J. Chem. Phys.* **1984**, *81*(8), 3684.
- [25] M. Parrinello, A. Rahman. *Phys. Rev. Lett.* **1980**, *45*(14), 1196.
- [26] V. E. Bahamonde-Padilla, J. J. López-Cascales, R. Araya-Maturana, M. Martínez-Cifuentes, B. E. Weiss López. *Chem. Phys. Chem.* **2014**, *15*(7), 1422.
- [27] T. Seiji, M. Yoshida, T. Uchimaru, M. Mikami. *J. Phys. Chem. A* **2001**, *105*(4), 769.

**How to cite this article:** Muñoz-Gacitúa D, Garrido C, Ruiz-Fernández A, et al. Molecular dynamics characterization of silver colloidal interfaces for SERS applications. Gallic acid test. *J Raman Spectrosc.* 2018;49:256–261. <https://doi.org/10.1002/jrs.5274>